

Quality Measurement Techniques for Hot-rolling Rolls[†]

TAKADA Hajime^{*1} YAMAMOTO Katsushi^{*2} HIRAOKA Hisashi^{*3}

Abstract:

This paper describes state-of-the-art nondestructive testing techniques developed at JFE steel for the hot-rolling of steel sheets. The following are reported: (1) A technique for high-resolution ultrasonic detection of internal flaws in deep positions through a combination of focused beam testing and a synthetic aperture method; (2) A technique for detecting surface flaws with a high signal-to-noise ratio using a newly developed broad-bandwidth surface wave probe; (3) An intelligible display technique for mapping the flaws detected in the surface testing. The development of these techniques has made it possible to thoroughly evaluate the soundness of work-rolls. The techniques are now being applied to actual production processes to maintain a high surface quality for sheet steel and to prevent work-roll troubles caused by internal flaws and surface flaws.

1. Introduction

Work rolls are repeatedly subjected to high stress while being used for the hot-rolling of steel sheets. Surface flaws are occasionally formed in work-rolls used for rolling under abnormal rolling conditions. When a surface flaw remaining in a work-roll is repeatedly subjected to high stress, it can expand into a large crack and thereby cause problems such as roll spalling and marking on the rolled strip. To cope with the wear and roughening of the work-roll, the surface of the work-roll is ground by a grinder after rolling a prescribed length of strip. Once re-profiled by the grinder, the surface of the work-roll is tested by a surface flaw detector. If a surface flaw is detected, the surface is re-ground until the sur-

face flaw is removed. In addition, small internal cracks can cause problems. When such a crack appears around a small internal flaw, it may grow into a big crack with repeated high stress.

The only reliable way to maintain the surface quality of a steel sheet and to prevent the work-roll troubles induced by surface flaws and internal flaws is to use the work-roll with no surface flaw and no internal flaw. It needs the detection of both surface flaws and internal flaws with high certainty. JFE has therefore developed several nondestructive testing techniques to thoroughly evaluate the soundness of work-rolls. This paper outlines the techniques developed by JFE.

2. High-resolution Ultrasonic Detection of Internal Flaws in Deep Positions by Combining Focused Beam Testing with a Synthetic Aperture Technique

A work-roll for the hot-rolling of steel sheets consists of an outer layer (a maximum of 80 mm in thickness) that comes into direct contact with the material to be rolled and an inner layer coupled to a drive shaft. The region between the surface of the outer layer and the boundary between the two layers needs to be tested precisely. When a small internal crack appears near an internal flaw, the dispersion and shape of the flaw will determine whether the crack will grow into a big crack when repeatedly subjected to high stress. Therefore, the method used for detecting internal flaws must be capable of detecting the dispersion and shape of small internal flaws existing at depths of up to 80 mm from the surface. JFE has developed the technique described below

[†] Originally published in *JFE GIHO* No. 15 (Feb. 2007), p. 32–37



^{*1} Senior Researcher General Manager,
Instrument and Control Engineering Dept.
& Plant Risk Forecast Project,
JFE R&D



^{*2} Staff Deputy Manager,
Hot Rolling Plant Control Sec.,
Plant Control Dept.,
East Japan Works(Chiba),
JFE Steel



^{*3} Manager, Casting Technology Sec.,
Manufacturing Dept.,
Chita Works,
JFE Steel

and is now applying it for the detection of internal flaws in work-rolls.

2.1 Ultrasonic Beam Focusing in Deep Position of Test Object

The immersion testing method with a focused ultrasonic beam is regarded as the most effective among the conventional methods for internal flaw detection. As shown in Fig. 1, the interior of the work-roll can be tested by scanning an ultrasonic focused probe in the axial direction of a rotating roll immersed in water. The probe transmits and receives ultrasound in the direction normal to the roll surface. This technique, however, has a limit.

The near field distance x_0 is written as

$$x_0 = D^2/4\lambda \dots\dots\dots (1)$$

where λ is the wavelength of ultrasound, D is a diameter of a cylindrical piezoelectric element¹⁾.

A piezoelectric element is considered to be a collection of many small elements. Without a means for focusing, such as an acoustic lens or curving of the piezoelectric element, the phases of the ultrasound radiated from respective elements coincide with each other at the near field distance (natural focus). For this reason, the focal length of the focused beam needs to be shorter than the near field distance x_0 in order to obtain a good focusing gain. Practically speaking, the focal length F of the focused beam needs to be shorter than $x_0/2$. In the ultrasonic testing of a large-size object such as a work-roll, ultrasonic waves of 1 to 2 MHz in frequency are commonly used to reduce attenuation resulting from scattering at grain boundaries. Since the maximum element diameter of the focused probe commonly used in the frequency range mentioned above is smaller than 30 mm, x_0 is shorter than 300 mm in water and shorter than 75 mm in steel. In reference to the description above, the material making up the outer layer of a hot-rolling work-roll is usually something like steel. Therefore, it is impossible to form the focus at a position 80 mm in depth from the surface of an object made of steel.

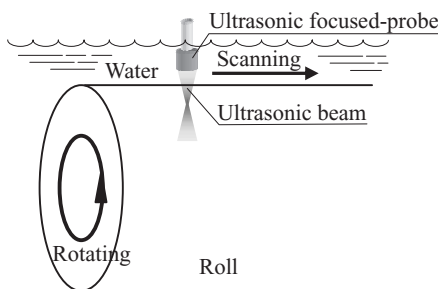


Fig. 1 Roll internal testing using ultrasonic focused probe

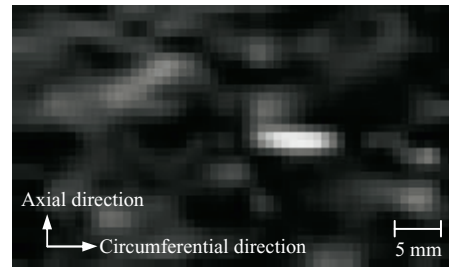


Fig. 2 C-scan image of a flat-bottom hole 1 mm in diameter and 80 mm in depth

Accordingly, we prepared a geometric framework to consider the matter on the basis of Eq. (1). Concluding that a larger element diameter was effective, the authors prepared focused probes of 50 to 75 mm in diameter using a piezoelectric material with an electrical impedance that would not fall to an unduly low level as a result of the larger diameter. A focused probe of 50 mm in diameter with 2 MHz in frequency, for example, can form the focus at a position 80 mm in depth, since x_0 of the probe is longer than 830 mm in water and longer than 200 mm in steel.

Figure 2 shows the detection result for a flat bottom hole (FBH) of 1 mm in diameter existing at a depth of 80 mm in a steel block set into a work-roll. The 50 mm-diameter focused probe with the 2 MHz in frequency was used for the detection, and the focal point of the focused beam was set to the 80 mm in depth. This experiment verified that the 1 mm-diameter FBH could be detected with a high signal-to-noise ratio. The image of the FBH was vague and distorted, however, because of the limitation on the beam diameter at the focal point and the deviation between the focal point in the circumferential cross section and the focal point in the axial cross section.

2.2 High-resolution Imaging Method

Having failed to visualize the internal flaw in sufficient detail using only the large-diameter focused probe, the authors searched for a method to obtain a higher resolution. Eventually we developed the synthetic aperture technique with an immersion focused transducer (SwiFT)²⁾. This method achieves high resolution by combining echo-signals obtained in immersion focused beam testing with an imaging method based on the synthetic aperture technique. An outline of this technique follows. The value of the counter $C_{k,l}$ after the procedure mentioned below shows the probability that a small element $PF_{k,l}$ is the source of echo signals. The map of the counted value can be interpreted as an image of the flaw.

- (1) The focal point of the focused beam is set to the depth position to be tested.
- (2) Flaw-echo signals are recorded at each measuring point $P_{i,j}$ in the test surface (See Fig. 1 and Fig. 3) by

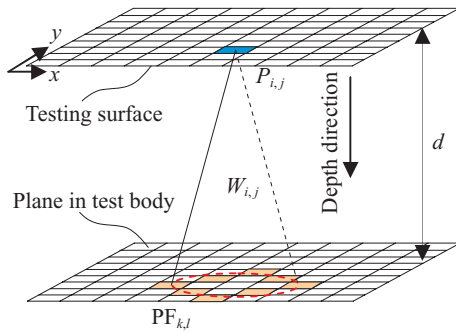


Fig. 3 Flaw image reconstruction method based on synthetic aperture method

2-dimensional scanning of the ultrasonic probe. The beam path length $W_{i,j}$ of the echo is calculated using the time difference between the surface-echo and the flaw-echo.

- (3) The depth position d where the flaw is estimated to exist is calculated. Each element in the plane with the depth of d is 2-dimensionally addressed by $PF_{k,l}$.
- (4) Distances L between the measuring point $P_{i,j}$ and all the elements $PF_{k,l}$ are calculated, and if $L=W_{i,j}$, 1 (one) is added to the counter $C_{k,l}$.
- (5) The procedure mentioned in (4) is executed for every measuring point $P_{i,j}$

2.3 Imaging of Internal Flaws in a Cut-out Sample Using SwiFT

Internal flaws positioned at a depth of 80 mm in a test block cut out of a large-size cast steel product were tested using SwiFT and a conventional method for immersion focused beam testing. The experiments were performed with the 50 mm-diameter focused probe with a 2 MHz frequency, with the focal point of the focused beam set to 80 mm in depth. **Figure 4** compares the image (the brightness is modulated according to the probability) of internal flaws obtained by SwiFT and a C-scan image (the brightness is modulated according to

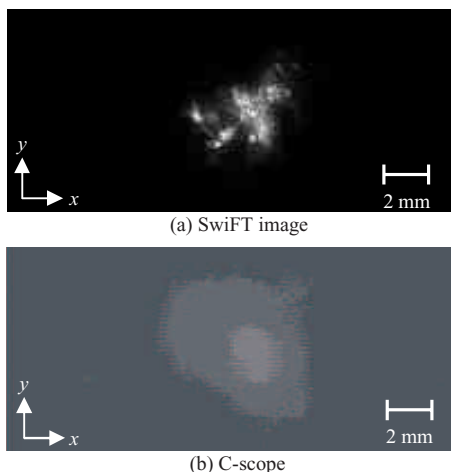


Fig. 4 Comparison between SwiFT image and C-scope

the echo amplitude) of the same internal flaws obtained using of the conventional method for immersion focused beam testing. The resolution obtained by SwiFT was superior beyond comparison. The image of the internal flaws agreed well with the metallographic image in the cross-sectional observation.

3. Roll Surface Testing

Using Broad-bandwidth Surface Waves

3.1 Problems in Conventional Technique and Background for Development

The work-rolls used for hot finish rolling are usually made of high-speed tool steel and their surfaces tested by surface wave testing³⁻⁶. The whole surface of the work-roll (test body) is tested by scanning a surface wave probe in the axial direction of the rotating roll as shown in **Fig. 5** (in **Fig. 6** this scanning is described as a “helical scan”). The probe transmits the surface wave in the direction opposite to the rotation of the roll and receives surface flaw echoes. A water-gap method is used for the coupling between the surface wave probe and the test body⁷.

In the surface testing of the work-roll, the presence of coarse grains, a rough surface, and a profusion of minute fine cracks produced in hot rolling (hereafter described as “collective fine reflectors”) produce back-scattered waves with small amplitudes. When these back-scattered waves superimpose with each other during conventional

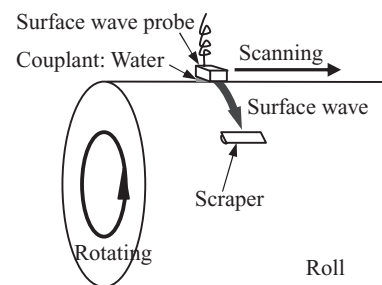


Fig. 5 Roll surface testing by use of surface waves

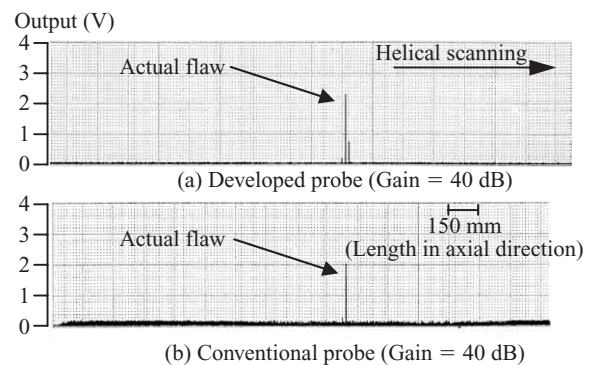


Fig. 6 Comparison of the test results of roll with an actual surface flaw 7 mm in length (inclined shape)

techniques, they collectively produce large amplitudes and the following problems result: (1) in some cases, the deteriorated signal-to-noise ratio of the flaw echoes makes it impossible to detect surface flaws, and (2) back-scattered waves with high amplitudes create the false appearance of flaws (false indication) where none are present.

3.2 Development of a Broad-bandwidth Surface Wave Probe with High Sensitivity

The height P_g of echoes from the collective fine reflectors in the path of ultrasound is give by

$$P_g = \sqrt{a_0 \cdot \tau} \cdot \exp(-2a_0x)/x \dots \dots \dots (2)$$

where, x is a distance from the probe to the reflector and a_0 is the attenuation coefficient, a value proportional to the square root of the pulse duration τ of the ultrasound⁸⁾.

From Eq. (2), the authors see that a shortening of the pulse duration of ultrasound effectively reduces P_g . Because the reflectivity of ultrasound at a flaw is independent of the pulse duration of the ultrasound, the authors can increase the signal-to-noise ratio of a flaw echo using a broad-bandwidth probe. Thus, the authors can also raise the detectability using a broad-bandwidth probe. The duration τ of the ultrasound pulse in the conventional technique is several times longer than the wavelength of the pulse, since the conventional surface wave probe obtains high sensitivity by sending out the oscillation of the piezoelectric element without damping. Therefore, P_g has a large value in the testing with the conventional narrow-bandwidth probe.

When using a broad-bandwidth probe, a short pulse is obtained by damping the oscillation of the piezoelectric element with a damping block. This drastically reduces the sensitivity of the broad-bandwidth probe in transmission and receiving, compared to a narrow-bandwidth probe. The gain of the receiving amplifier needs to be set at a high value to compensate for the decline in sensitivity, which increases the likelihood of misdetection of electrical noises in the air.

JFE developed a broad-bandwidth probe with a higher sensitivity than the conventional narrow-bandwidth probe. The following improvements in the probe made this possible.

(1) Selection of Materials

(Piezoelectric Element, Resin Wedge)

To obtain high sensitivity and to lower the amplitude of spurious echoes, a piezoelectric element with a high electro-mechanic coupling factor in the thickness direction and low electro-mechanic coupling factor in the radius direction is used as the oscillator for the ultrasound. A resin with low ultrasound

attenuation and high acoustic impedance is used as the wedge material.

(2) Modification of the Incident Angle

The incident angle θ_i from the wedge to the roll surface is determined on the basis of the surface wave velocity in the high-speed tool steel, in order to satisfy Snell's law.

3.3 Performance and Utility of the Newly Developed Probe

Photo 1 compares the waveform of the surface wave transmitted by the newly developed probe with the waveform of the surface wave transmitted by the conventional surface wave probe. The newly developed probe with the center frequency of 2 MHz and pulse duration with a 1.5 wavelength is 8 dB more sensitive than the conventional probe⁹⁾.

Photo 2 shows test results using an artificial surface flaw of 0.2 mm in depth and 0.5 mm in width engraved by electro-discharge machining in a high-speed-steel plate of 10 mm in thickness. The probe was set at a distance of 100 mm from the artificial flaw. The signal-to-noise ratio of the flaw echo observed using the newly developed probe was about 10 dB higher than that observed using the conventional narrow-bandwidth probe. Test results using artificial surface flaws with the newly developed probe have proved that surface flaws with cross sections above 0.06 mm² can be detected with a signal-to-noise ratio beyond 10 dB. With the conven-

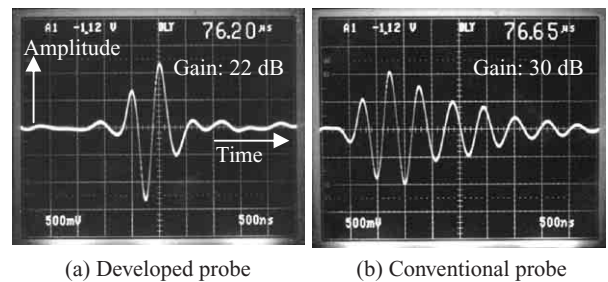
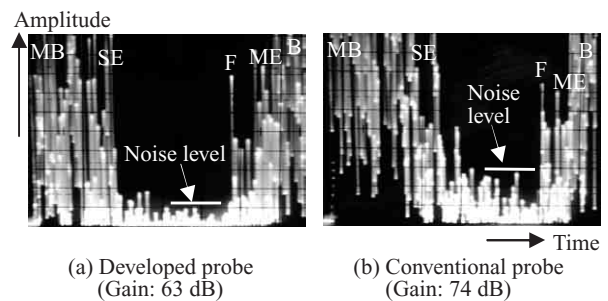


Photo 1 Waveforms of side wall echoes



MB: Main bang, F: Flaw echo, B: Edge echo, SE: Spurious echo in wedge, ME: Mode converted echo

Photo 2 Test results of an artificial surface flaw detection

tional narrow-bandwidth probe, artificial flaws must have cross sections of at least 0.2 mm^2 to be detected. Thus, the newly developed probe can detect a flaw with a cross section three times smaller than the smallest cross section detectable by the conventional narrow-bandwidth probe.

Figure 6 shows the results of flaw detection tests with the newly developed probe and the conventional narrow-bandwidth probe installed in an automatic roll surface flaw detector, using a work-roll with a crack formed during rolling. The height of the crack echo detected with the newly developed probe was equal to that detected with the conventional probe, whereas the height of the noise detected with the newly developed probe was much lower than that detected with the conventional probe. This confirms that cracks can be detected with a high signal-to-noise ratio using the newly developed probe.

4. Intelligible Display Technique for Mapping Flaws Detected in Surface Testing

Another important requirement for reliably preventing work-roll troubles is a system to display the detected flaws with high clarity and easy operability. Therefore, the authors also developed an improved display technique for mapping the detected flaws in surface testing.

4.1 Conventional Display Techniques and Their Shortcomings

There are two conventional methods for displaying detected flaws. One uses an oscillograph to record analogue voltages which are proportional to the amplitudes of the flaw signals (analogue-voltage-recording method). The other system detects positions where flaw signals exceed the predetermined threshold voltage, and displays them using symbols in a map of the roll developed using records of the flaw signal and the test position obtained in surface testing (symbol-on-map display method).

Figure 7(a) shows an example of the analogue-voltage-recording method and Fig. 7(b) shows an example of the symbol-on-map display. Figure 7 shows the results of surface wave testing of a roll with artificial flaws. In Fig. 7(b), the detected flaw is classified into three categories by comparing the amplitude of the flaw signal with three thresholds (L , M , H , $L < M < H$). A flaw with a signal amplitude larger than the L threshold and smaller than the M threshold is classified as an L flaw. A flaw with a signal amplitude larger than the M threshold and smaller than the H threshold is classified as an M flaw. A flaw with signal amplitude larger than the H threshold is classified as an H flaw.

The advantages and disadvantages of the two display

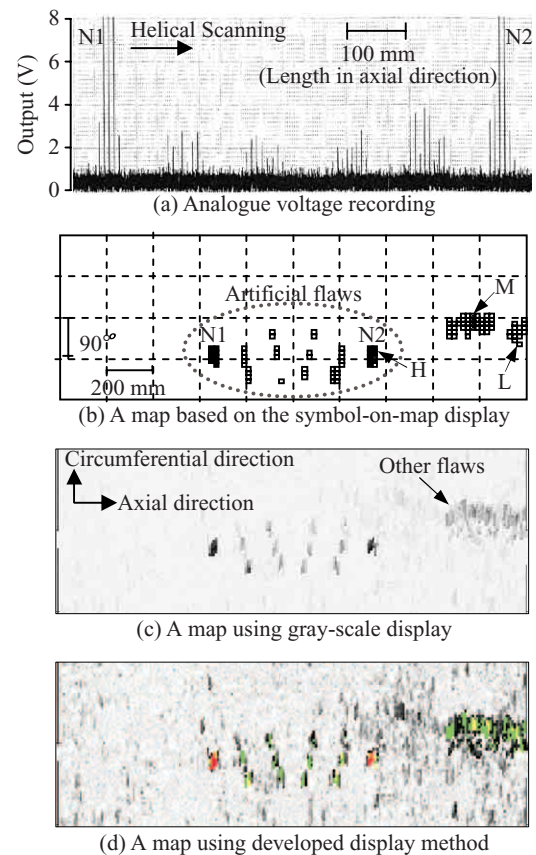


Fig. 7 Comparison between a map displayed by the newly developed display method and maps displayed by conventional display methods

methods are diametrically opposed. The symbol-on-map display can be easily used to grasp the flaw position, but cannot display a surface flaw with an amplitude smaller than the threshold. In contrast, the analogue-voltage-recording method fails to indicate the flaw position but succeeds in recognizing a surface flaw with a small signal amplitude. In this connection, an excessively reduced threshold L in the symbol-on-map method leads to occasional false detection due to electrical noises, grass echoes arising from the grain and rough surface, and superposition of electrical noises and grass echoes.

One workable option may be to apply a conventional display technique for displaying C-scan images by expressing the amplitudes of the flaw signals with gray scaling or coloring (ordinary C-scope display method). When a detected flaw has a higher signal level than a pre-determined threshold, however, it must be removed by grinding after the roll surface testing. Therefore, the display system must distinctly show this flaw when the signal level of detected flaw exceeds the pre-determined threshold. The ordinary C-scope display method is thus unusable in this case, as the method will not readily recognize the signal level of detected flaws.

4.2 New Method for Displaying Detected Flaws

JFE has developed a new display method with

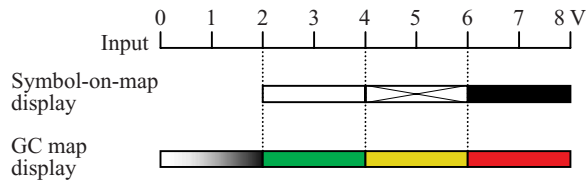


Fig. 8 Comparison of displaying map methods for the signal amplitude

the advantages of both of the conventional methods described above (the analogue-voltage-recording method and symbol-on-map display method)¹⁰. In the new coloring method mentioned below, distinct color combinations with different tones such as a grayscale and colors (e.g., red, green, blue) can be easily discriminated. A signal with an amplitude below a pre-determined threshold is colored by grayscale according to the amplitude, and a signal with an amplitude above a pre-determined threshold is colored using clear colors (GC map display method). **Figure 8** shows the difference between the GC map display and the symbol-on-map display.

4.3 Comparison between Display Methods

Figures 7(b), 7(c), and 7(d) show surface testing results of a roll with artificial flaws displayed using the symbol-on-map display, 64-gradations gray-scaling, and a GC map display, respectively. Figure 7(b), the symbol-on-map display, shows no artificial flaws with signal amplitudes lower than the pre-determined threshold. In Fig. 7(c), the map display with 64-gradation gray-scaling, the flaws with low signal amplitudes are displayed with low contrast, difficult to identify, and difficult to distinguish from each other. In Fig. 7(d), the GC map display, the flaws with low signal amplitudes are displayed with high contrast and relatively easy to grasp.

4.4 Examples of Maps Displayed by the GC Map Display Method

Figure 9 shows the change in the surface testing results induced by grinding, by comparing maps displayed using the GC map display method. Figure 9(a) shows the surface testing result after the roll was taken out from a hot-rolling mill and ground normally according to schedule. The system detected a surface flaw with a signal amplitude higher than threshold L , hence the roll was ground again. As shown in Fig. 9(b), the signal amplitude of the surface flaw was reduced to below threshold L by re-grinding, but dark gray marking remained at the same position. The surface flaw appeared to be unexpectedly deep. Remaining surface flaws such as this may cause roll trouble. The symbol-on-map display did not display the surface flaw remaining in the re-ground surface. As a conclusion, the GC map display method clearly identified both the signal

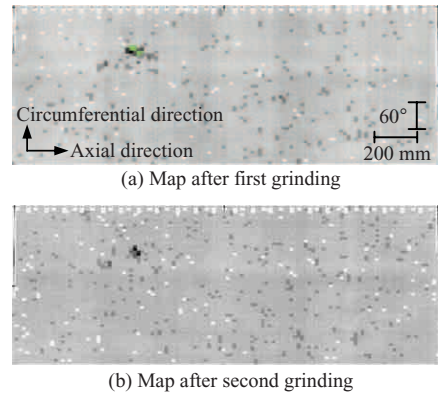


Fig. 9 Change in surface testing results in the process of surface grinding

amplitude and the position of the surface flaw detected with a signal amplitude lower than the threshold.

5. Conclusion

The following nondestructive testing techniques for work-rolls have been developed at JFE Steel: (1) a surface flaw detection technique with a high signal-to-noise ratio using a newly developed broad-bandwidth surface wave probe; (2) an intelligible display technique for mapping flaws detected in the surface testing; (3) a high-resolution ultrasonic detection technique for detecting internal flaws in deep positions by combining immersion focused beam testing with a synthetic aperture technique. These techniques have made it possible to evaluate the soundness of work-rolls thoroughly, and their application to actual production processes has helped to maintain a high surface quality for sheet steel and prevent work-roll troubles caused by internal flaws and surface flaws.

References

- 1) The Japanese Society for Non-Destructive Inspection Ultrasonic Testing III. The Japanese Society for Non-Destructive Inspection, Tokyo. 2001, p. 57. (Japanese)
- 2) Takada, H.; Hiraoka, H.; Yamashita, Y. CAMP-ISIJ. 2005, vol. 18, p. 337. (Japanese)
- 3) Ando, Y.; Sorano, H.; Sano, Y. CAMP-ISIJ. 1992, vol. 5, p. 515. (Japanese)
- 4) Ekusa, T.; Komiya, T.; Yonezawa, Y.; Ohniwa, A.; Murai, J. CAMP-ISIJ. 1994, vol. 7, p. 358. (Japanese)
- 5) Tsuchiya, Y.; Ohnishi, R.; Kodoi, A.; Shiraiishi, K.; Masuda, K.; Okimoto, K. CAMP-ISIJ. 1993, vol. 6, p. 505. (Japanese)
- 6) Sorano, H.; Morino, Y.; Sano, Y. CAMP-ISIJ. 1996, vol. 9, p. 984. (Japanese)
- 7) Japanese Unexamined Patent Publication 7 294493. (Japanese)
- 8) Ermolov I.N. NDT Int. vol. 9, 1976-12, p. 275-280.
- 9) Takada, h.; Torao, A.; Yarita, I.; Sugimoto, R.; Ogawa, H.; Morii, T.; Sato, A.; Akazawa, H. CAMP-ISIJ. 1999, vol. 12, p. 897. (Japanese)
- 10) Yamamoto, K.; Maeda, I.; Sugimoto, R.; Takada, H. CAMP-ISIJ. 2000, vol. 13, p. 1044. (Japanese)